Embryonic Fibroblast Motility and Orientation Can Be Influenced by Physiological Electric Fields

CAROL A. ERICKSON and RICHARD NUCCITELLI
Zoology Department, University of California, Davis 95616

ABSTRACT Epithelial layers in developing embryos are known to drive ion currents through themselves that will, in turn, generate small electric fields within the embryo. We hypothesized that the movement of migratory embryonic cells might be guided by such fields, and report here that embryonic quail somite fibroblast motility can be strongly influenced by small DC electric fields. These cells responded to such fields in three ways: (*a*) The cells migrated towards the cathodal end of the field by extending lamellipodia in that direction. The threshold field strength for this galvanotaxis was between 1 and 10 mV/mm when the cells were cultured in plasma. (*b*) The cells oriented their long axes perpendicular to the field lines. The threshold field strength for this response for a 90-min interval in the field was 150 mV/mm in F12 medium and between 50 and 100 mV/mm in plasma. (*c*) The cells elongated under the influence of field strengths of 400 mV/mm and greater. These fibroblasts were therefore able to detect a voltage gradient at least as low as 0.2 mV across their width. Electric fields of at least 10-fold larger in magnitude than this threshold field have been detected in vivo in at least one vertebrate thus far, so we believe that these field effects encompass a physiological range.

The directional movement of cells during embryogenesis, wound healing, and tumor invasiveness has been well documented (42, 43). In particular, there are many instances when embryonic cells migrate as individual cells during embryogenesis and consistently follow a precise pathway toward their final destination (e.g., neural crest, precardiac mesenchyme, primordial germ cells, and lateral movement of mesoblast away from the primitive streak, to name a few). The mechanisms behind this behavior remain obscure. Several candidates have been proposed and include extrinsic influences such as contact inhibition, contact guidance, chemotaxis, and differential adhesiveness (haptotaxis) as well as intrinsic factors programmed within the cells. One less explored environmental factor that might guide cell movement is an electric field. Embryonic electric fields can be generated by ion currents driven into the embryo by the epithelium which is well known to pump in positive ions such as Na^+ (23). Such embryonic currents have already been measured exiting the primitive streak of chick gastrulae (20) and the blastopore of frog neurulae (36) in addition to eminating from the cut surface of wounds (3) and regenerating limbs (5), where morphogenesis is also occurring. Furthermore, there is good evidence from tissue culture studies that some cells, such as amoebae (44, 37), macrophages (31), leukocytes (9, 14), and slime molds (1), show sensitivity to imposed electrical fields by displaying a galvanotactic response. Recently, a related phenomenon of embryonic cell galvanotropism has also been observed in developing neurons. This cell type grows toward the cathode in a DC electric field (19, 16, 13, 33). It is important to note that the field strengths that elicit these galvanotropic and galvanotactic responses in vitro are quite small and may well be generated in vivo.

We have been particularly interested in the role of electric fields in guiding morphogenetic movements of individual embryonic cells and have previously demonstrated that quail somitic fibroblasts and quail neural crest cells display a striking sensitivity to electric fields as low as 150 mV/mm by orienting perpendicular to the field and migrating towards the cathode (12, 30). Three other labs have recently observed similar galvanotaxis behavior in neural crest and epithelial cells (7, 40, 26). In this paper we describe in detail the behavior of somite fibroblasts in a imposed electric field under a variety of experimental conditions. Here we report a much lower threshold than previously reported for the galvanotaxis response of between 1 and 10 mV/mm in plasma. We chose somitic sclerotome cells for these studies since they initially

THE JOURNAL OF CELL BIOLOGY · VOLUME 98 JANUARY 1984 296-307
 · 0021-9525/84/01/0296/12 $1.00

undergo a directed ventral dispersion around the neural tube during development. For a review of the directed movements of embryonic fibroblasts, see Trinkaus (43).

MATERIALS AND METHODS

Cell Culture

Cell cultures were established as previously described (25). Briefly, neural tubes and associated tissues were excised from 22-somite quail embryos (*Coturnix coturnix japonica*) and digested with full-strength pancreatin (Gibco Laboratories, Grand Island, NY) until all somitic, notochordal, and epithelial tissues could be dissected away with sharpened tungsten needles. Somites were cut into pieces, transferred onto acid-washed 22 × 9-mm coverslips (Gold Seal Clay Adams, Parsippany, NJ), and grown in F12 medium (Gibco Laboratories) containing 10% fetal calf serum and 3% chick embryo extract. The cells were allowed to spread on the coverslip for 48 h in a 5% CO_2 incubator at 37°C before placing them in our experimental chamber for study.

Experimental Protocol

Immediately before each experiment, the coverslip containing the cells was washed 3 × in F12 medium containing 10 mM HEPES buffer, but no serum or embryo extract. The coverslip was then placed in a specially designed chamber (Fig. 1 *a*), which consisted of a 45 × 50-mm coverslip glass bottom onto which two 6 × 25-mm pieces of no. 2 coverslip were waxed to form a 9-mm wide trough. The no. 1 coverslip with cells on it was placed in this trough which was filled with the protein-free F12 medium (pH 7.0) and sealed with a coverglass and silicon high-vacuum grease (Dow Corning Corp., Midland, MI) to prevent desiccation. The fluid height over the cells varied from 90 to 180 μm, depending on the thickness of the wax layer. Heights >200 μm or <90 μm resulted in unacceptable levels of cell death. For the cross-current fluid flow experiments the chamber was modified as shown in Fig. 1 *b* so that two troughs were formed, allowing us to pass fluid over the cells perpendicular to the electric field lines. Chambers were maintained at 37°C with an air curtain incubator (Sage model 279, Sage Instruments Div., Orion Research, Inc., Cambridge, MA) during the experiments. Direct current (DC) was applied through Ag-AgCl electrodes immersed in saline-filled wells that were connected in turn to the chamber wells by 10-cm long 2% agar bridges. Current was measured continuously with a Keithley model 600B electrometer (Keithley Instruments, Inc., Cleveland, OH) and the voltage across the chamber was measured directly with a voltmeter by inserting Ag-AgCl electrodes into the ends of the chamber trough at the beginning and end of each experiment. This direct voltage measurement provided the field strength values reported here. We find that this is more accurate than a calculation of the field strength based on the current and chamber cross-sectional area which usually yields for unknown reasons a value approximately twofold larger than the actual field strength. The cells were observed with a Nikon Diaphot inverted microscope, and their behavior was recorded with an RCA video camera and a Panasonic time-lapse video tape deck. After each experiment, cultures were fixed with 2.5% glutaraldehyde in 0.1 M NaCacodylate buffer and photographed.

The above experimental protocol was varied in several ways. Occasionally, either Hanks' basic salt solution (HBSS) containing 10 mM HEPES buffer, or chicken plasma (Gibco Laboratories) diluted 1:1 with F12-HEPES, was substituted for F12 medium in the chamber. The plasma was diluted to prevent clotting. In other experiments the cells were embedded in a hydrated collagen lattice prepared exactly as described by Elsdale and Bard (11). In some experiments the modified chamber of Fig. 1 *b* was used so that a cross-current fluid flow could be imposed on the cells. All figures describe experiments done in F12 medium unless noted otherwise in legend.

Quantitation of Cell Behavior

DIRECTED MOTILITY: The direction of movement and other behavioral responses to the electric fields were determined from video tapes. Direction and speed of movement were measured by tracing the position of cell nuclei every 10 min from the video screen onto acetate sheets. The direction of lamellipodium extension and cell retraction were also ascertained by observing these time-lapse recordings.

PERPENDICULAR ALIGNMENT: The orientation of a cell with respect to the electric field was defined as a function of cos 2Θ, where Θ is the angle formed by the intersection of a line drawn through the long axis of each cell with a line drawn perpendicular to the field lines (Fig. 2). This polarization function was chosen for convenience since it varies on a scale from −1 to 1. A cell whose long axis is aligned perpendicular to the field lines will have a polarization of 1, and a cell whose long axis is perfectly aligned with the field will have a polarization of −1. Furthermore, a cell whose long axis is oriented at 45°, halfway between these extremes, will have a polarization of 0. Thus, a randomly oriented population of cells will have an average polarization (defined by $\Sigma_n \cos 2\Theta/N$) of 0. This average polarization was calculated for each experiment with the use of a digitizing tablet and computer. An 8 × 10-in photographic enlargement of a 40 × phase photomicrograph of the cells was placed on the digitizing tablet (Houston Instruments Hipad 191Z, Houston, TX) and the end points of the long axis of each cell were inputed to the computer. The average polarization for the cell population ($\Sigma_n \cos 2\Theta/N$) was then calculated and the significance of this two-dimensional orientation distribution against randomness was calculated using Rayleigh's distribution as described by Curray (7). The probability that the population is randomly oriented is given by $p = e^{-(L^2N\times10^{-4})}$ where $L = [(\Sigma_n \sin 2\Theta)^2 + (\Sigma_n \cos 2\Theta)^2]^{1/2}/N(0.01)$, and N is the total number of cells. We use a probability level of 0.01 as the limit for significant polarization. In most cases the polarization was measured before and after a 90-min exposure to an electric field, but in some experiments more frequent photographs were taken so that the time course of the cell orientatation response could be determined.

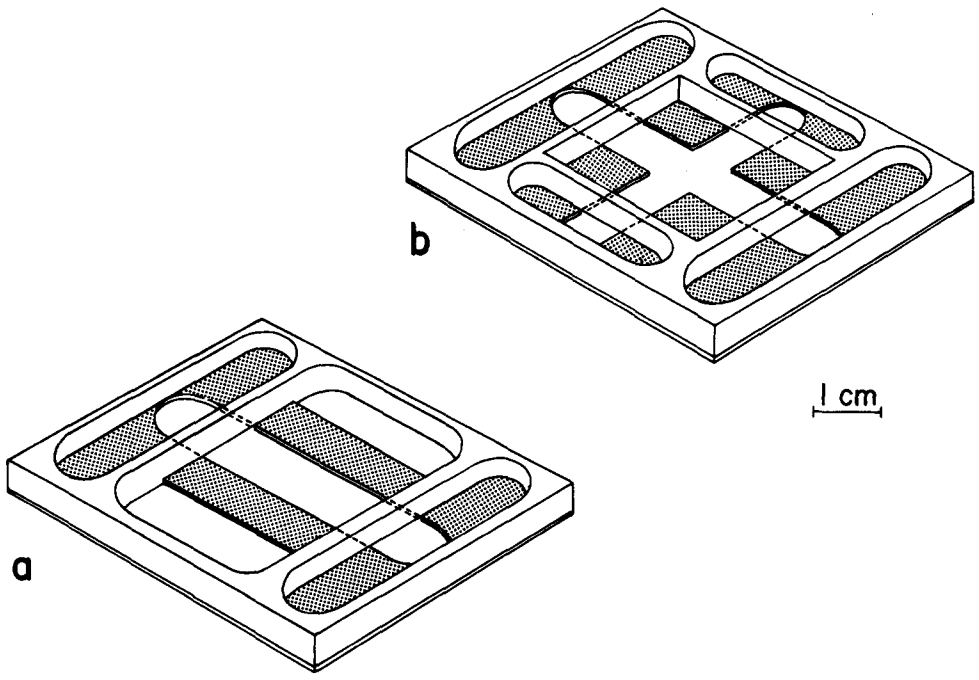

FIGURE 1 Experimental chambers used to apply the electric field to the cell cultures. The chamber bottom is a 45 × 50-mm piece of no. 1 ½ coverslip glass. A piece of 5-mm thick plexiglass was milled out to form the wells and waxed to the glass bottom. (*a*) Standard chamber that was used in most experiments. (*b*) Modified chamber that was used in the cross-current fluid flow experiments.

CELL ELONGATION: The cell length varies with the time of exposure to the field and with field strength. It was measured directly from the enlarged photographs with the aid of the digitizer and computer. There is a large standard deviation of ~25 μm when 300 cells are averaged, but significant differences in length could be detected under certain conditions.

RESULTS

We have previously reported that quail somite fibroblasts respond in three ways to an applied electric field (30). These are: (*a*) the cells migrate towards the cathodal end of the field; (*b*) the cells orient in the field so that their long axes are perpendicular to the field lines; (*c*) the cells also elongate under the influence of relatively high field strengths. We present here a detailed characterization of these responses.

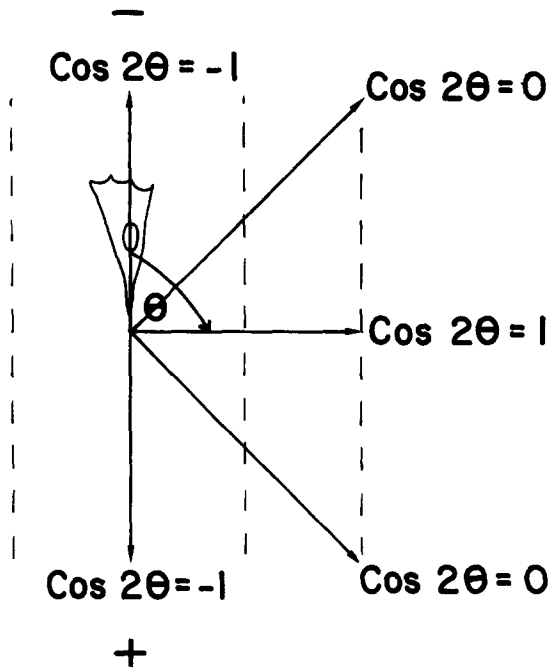

FIGURE 2 A drawing depicting the function used to quantitate orientation with respect to the field (i.e., polarization). Dashed lines represent electric field lines. Polarization is expressed as a function of cos 2Θ, where Θ is the angle that the long axis of a cell makes with a line drawn perpendicular to the field lines. Thus, a cell oriented perpendicular to the field lines will have a polarization value of 1; parallel to the field, a value of −1; and a value of 0 when oriented at a 45° angle to the field.

Directed Migration

The direction of cell migration was determined by tracing the movement of cell nuclei from the video screen at 10-min intervals. We first studied the effects of relatively large fields because the response was so dramatic. Cells in a 600 mV/mm field consistently moved toward the cathode (Fig. 3), whereas in control cultures the cells moved randomly in all directions. At progressively lower field strengths this response became steadily less pronounced (Fig. 4). However, even at the lower field strength of 200 mV/mm that produces minimal alignment of the cells perpendicular to the field lines (see below), significantly more cell migration was directed towards the cathode than towards the anode. In fact, we were surprised to find that the negative galvanotaxis could be easily detected at 10 mV/mm. The lower field of 1 mV/mm yielded significant negative galvanotaxis in three experiments and no significant galvanotaxis in three other experiments. Therefore, this field strength is probably very close to the threshold for this directed migration response. The average cosine of this distribution of migration directions ($\Sigma_n \cos \Theta/n$) is not significantly different from that measured in the absence of a field, whereas the average cosine for the 10 mV/mm case is clearly significantly different. When the current direction was reversed the cells stopped their cathodally directed movement and began migrating in the opposite direction (Fig. 5). This response to reversed fields is usually much faster and stronger than the response to the initial field, as if the cells had been "sensitized" by their previous exposure to the electric fields. This "sensitization" is quite important because it suggests that the cells may respond to even smaller fields after a short time in a field.

We studied this directional migration in more detail in the 600 mV/mm field and found that it can be accounted for by the fact that any new processes produced by the cells are always directed toward the cathode-facing side of the aligned cell (Fig. 6). The greatest percentage of these new processes

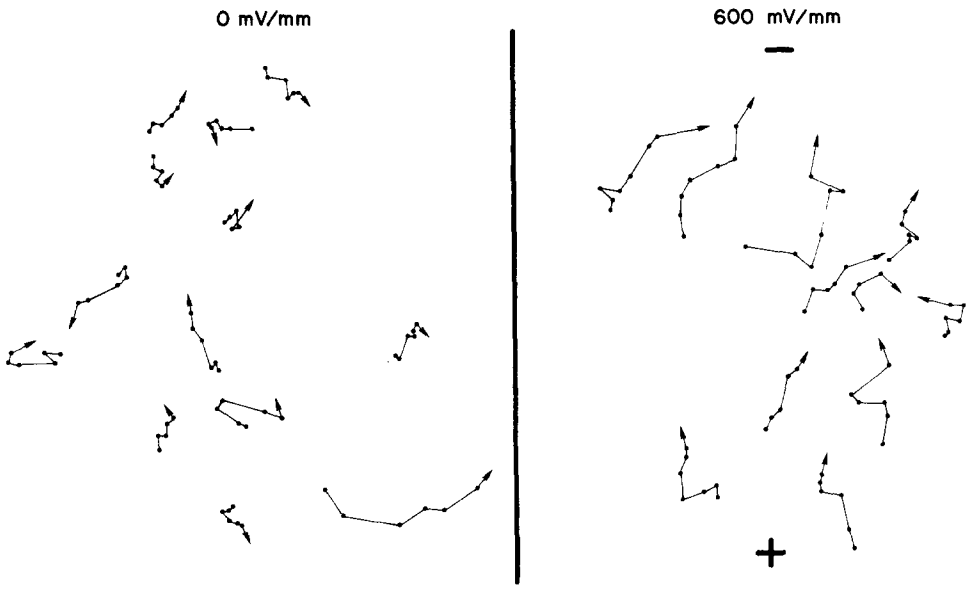

FIGURE 3 These tracings represent the pathways taken by fibroblasts in a control (*left*) and 600-mV/mm DC field (*right*). Each point represents the center of the nucleus traced every 10 min from the video screen. The anode and cathode are marked by + and −, respectively. The arrowheads indicate the last time point and consequently the direction of movement. Translocation appears random in the control culture, while the cells are all directed towards the cathode in the 600-mV/mm field.

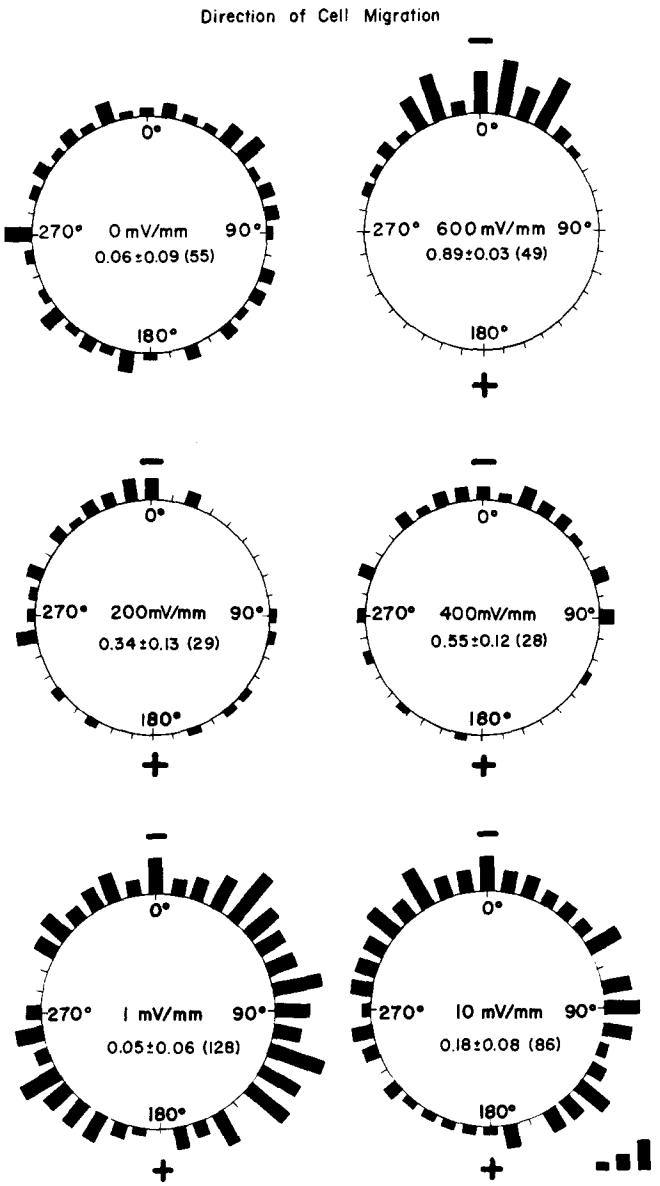

FIGURE 4 Histograms demonstrating the direction of cell migration during 90 min (120 min in the 1- and 10-mV/mm cases) in fields of varying strengths. 0° faces the cathodal end of a vertically directed electric field. The net migration direction was determined by drawing a line between the position of the cell nucleus before and after 90 min in the indicated field strength. The height of each bar is proportional to the number of cells observed to move in that direction and bar lengths representing one, two, and four cells, respectively, are on the lower right of the figure. The average cosine plus or minus SEM and total number of cells counted is indicated below the field strength value in each histogram. This average will be near 0 for a random distribution of migration directions and will be near 1 if most cells move toward the negative pole. Normally fibroblasts plated at low cell density migrate randomly (0 mV/mm). At 600 mV/mm, cathodally directed migration is striking. Even field strengths as low as 10 mV/mm result in predominant migration toward the negative pole. At 1 mV/mm there may be a slight migratory tendency towards the cathode, but this effect is only observed in half of the experiments and is not significant according to the average cosine and standard error. Experimental medium was chick plasma in 1 and 10 mV/mm.

were directed exactly towards the negative pole, but lamellipodia also extended throughout the 180° demarcated by the side of the aligned cell facing the cathode. These lamellipodia are unusual in that they were generally formed along the long sides of a cell so that the cells appeared to crawl sideways (Fig. 7). However, at field strengths below the 150 mV/mm threshold for the orientation effect (see below), the cells had the more traditional fibroblast morphology with the lamellipodium extending in the direction of migration and the long axis aligned with the direction of movement. The lamellipodia that formed in a 600 mV/mm-field were also quite changeable. For example, the center of such a process was frequently observed to cease protrusion so that eventually the lamellipodia extended only from either end of these elongate cells. These "canoe-shaped" cells still moved sideways towards the negative pole, since the processes at each end primarily extended toward the cathode. However, there was some stretching along the cell axis that resulted in the elongation response at higher fields.

The average speed of movement can also be influenced by the electric field. There was no significant change in this average speed for low field strengths of up to 300 mV/mm, but for 400 mV/mm and greater there was roughly a 40% increase in the average speed (Table I). Since this acceleration also occurred at the threshold for the retraction response, this increase in speed of movement may be due to retraction-induced spreading (6).

Orientation Response

ORIENTATION AT DIFFERENT FIELD STRENGTHS: Fibroblasts in control cultures or in cultures photographed before field application were randomly distributed with no predominant orientation of their long axes. This yields an average polarization very near zero as shown in Table II. Application of an external DC electric field resulted in a redistribution of the cells so that they tended to become oriented perpendicular to the field lines (Fig. 8). The greatest degree of alignment occurred at 600 mV/mm which produces an average polarization of 0.8 in ~60 min (a polarization value of 1 means that every cell is perfectly aligned perpendicular to the field). This field strength should produce a voltage drop of 12 mV across an average cell that is 20 μm wide, or 48 mV along its 80 μm length if its axis is aligned with the field. At decreasing field strengths the cells are progressively less aligned, and the lowest field strength that yielded a significant polarization in protein-free medium after 90 min was 150 mV/mm (Table II). However, for longer field applications of 3–4 h, significant polarization could be detected for 100-mV/mm fields (Table III).

This polarization response was also dependent on the medium used in the chambers. In chick plasma, for example, the cells again achieved maximum orientation at 600 mV/mm, but the threshold for a response was lowered to between 50 and 100 mV/mm for a 90-min exposure to the field (Fig. 9; Table II). The reason for this lower threshold is not known but it is worth noting that the cells appeared healthier under these conditions and that the plasma probably represented a more physiological medium for the cells.

CONTROL EXPERIMENTS: We conducted a variety of control experiments to be sure that the cells were responding to the electric field itself, and not to some field-induced environmental vector. It is very unlikely that the electric field produces a standing gradient of a culture medium protein, since the F12 medium used contains no serum or embryo extract. However, we also conducted these experiments in Hanks' saline which, unlike F12, is free of amino acids and

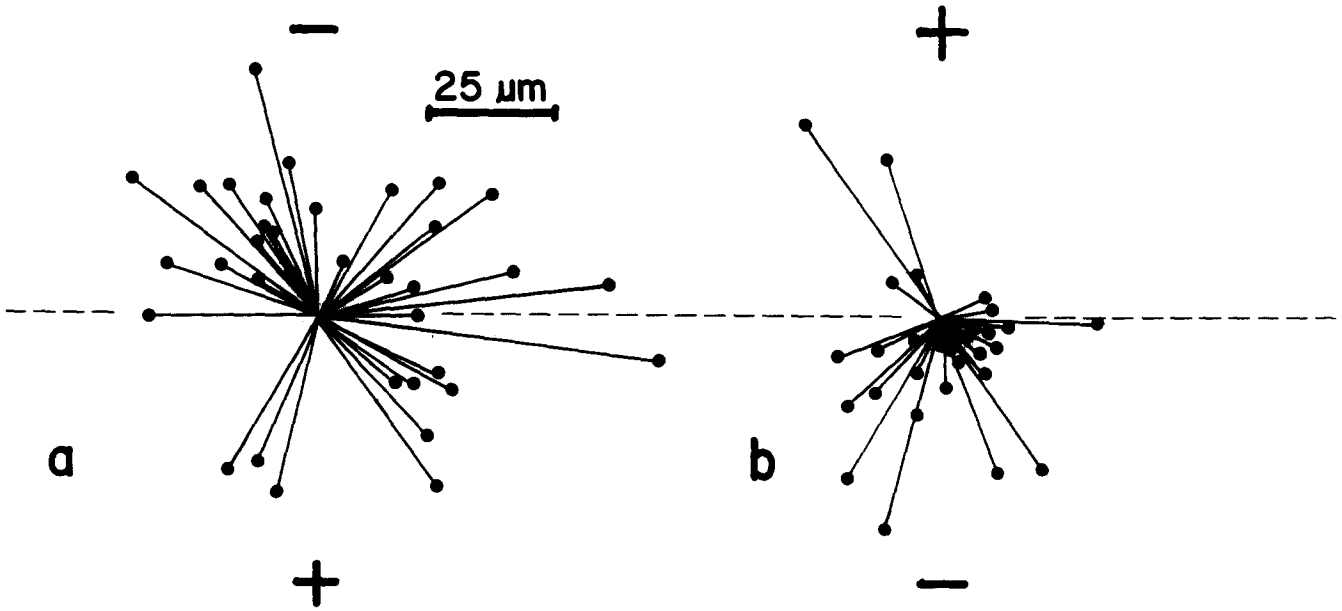

FIGURE 5 The distance and direction of fibroblast migration in a 10-mV/mm field was determined from videotapes of three experiments. (a) The vectors represent the distance and direction of movement over 2 h with the cathode at the top and the anode at the bottom of the diagram. The dotted line represents the boundary between the cathode and anode hemispheres. The majority of cells clearly migrate toward the negative pole. (*b*) The same fields of cells were observed for 1 h after the poles of electric field were reversed. The majority of cells have reversed their direction of migration and respond more rapidly to the reversed field as if they had been "sensitized" by the previous exposure to a field. Experimental medium was chick plasma.

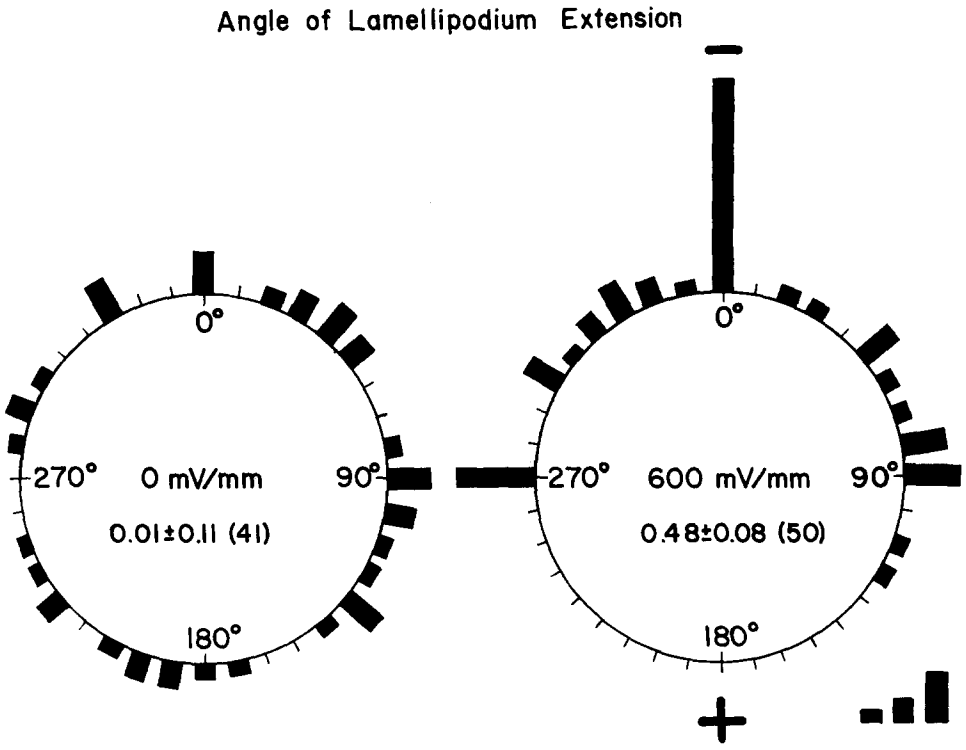

FIGURE 6 Histograms representing the direction of the initial lamellipodium extension after application of an electric field. 0° faces the cathodal end of the vertically directed field. The height of each bar is proportional to the number of processes measured and bar lengths representing one, two, and four cells, respectively, are given on the lower right of the figure. The average cosine of the distribution plus or minus the SEM and total number of cells counted is given below the field strength in each histogram. In controls, lamellipodia are extended randomly, but in the 600-mV/mm field all processes are directed towards the cathodal hemisphere, with the greatest percentage extended towards 0°. Note that many lamellipodia protrude perpendicular to the field and are apparently responsible for the elongation phenomenon observed at the higher field strengths.

is composed only of salts. The same orientation response was observed (Table III). It is unlikely that the cells themselves are producing some factor that is electrophoresed and influencing neighboring cells since an imposed fluid flow of 100 μm/s perpendicular to the field lines had no weakening effect on the response (Table III). Another control designed to reduce electro-osmotic fluid flow was to place the cells in a collagen gel. This eliminated the bulk fluid flow through the chamber as indicated by particle movement, but had very little effect on the orientation response at high field strengths (Table III). Finally, the application of alternating current was found to have no orienting effect. Fields of up to 1,200 mV/mm peak-to-peak at 60 Hz for 90 min produced no significant polarization (Table III; Fig. 8, *g* and *h*).

TIME COURSE OF ORIENTATION RESPONSE: The time course of the cell orientation response can be studied by analyzing sequential photographs of cell cultures during their exposure to electric fields. We found that in a 600 mV/mm-field the cells had already deviated significantly from a random orientation within 5 min of field application, although

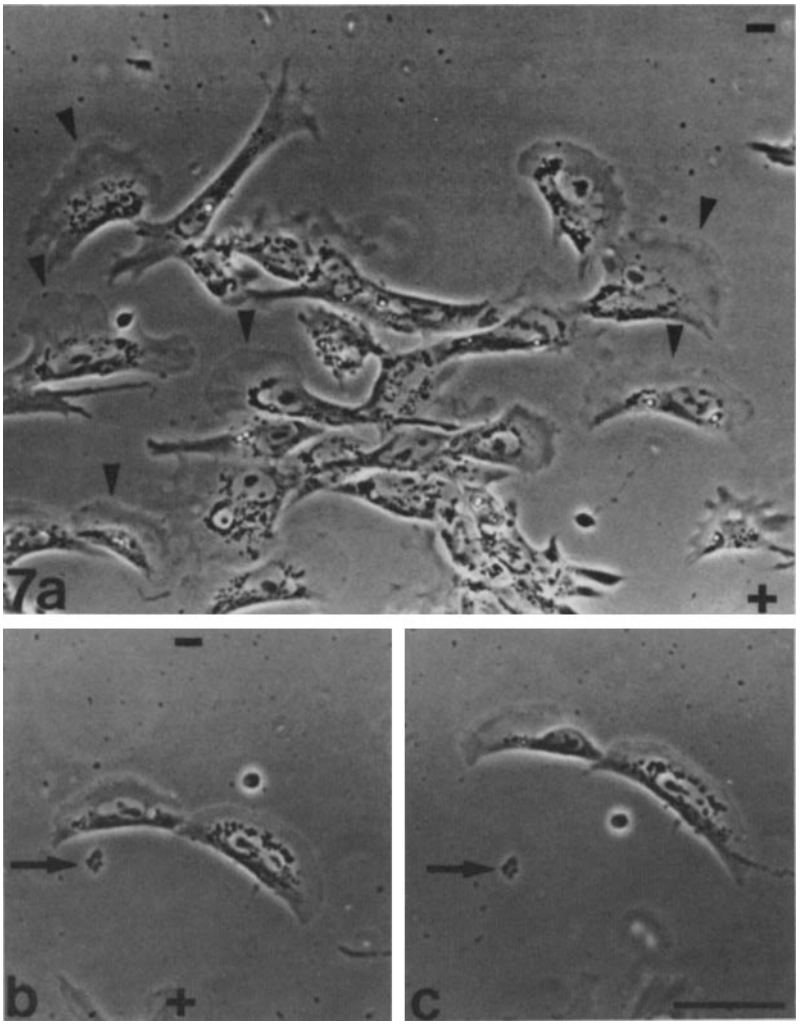

FIGURE 7 (*a*) Phase micrograph of fibroblasts after 90 min in a 600-mV/mm, vertically oriented field. The cathode is at the top of the micrograph. Note that even though the cells are oriented perpendicular to the field, all lamellipodia (arrowheads) extend from the sides of the cells toward the negative pole. (*b* and *c*) Two phase micrographs of the same cells photographed after 30 and 60 min, respectively, in a 600-mV/mm DC electric field. The cathode is at the top of the micrograph. The arrow marks a piece of debris that provides a fixed reference point. The cells have translocated nearly 50 μm towards the cathode in 30 min. Note that the cells are moving perpendicular to their long axis and that lamellipodia extend along their entire length. Bar, 100 μm. × 150.

the polarization was still quite small (0.13). Within 60 min the cell population had attained its maximium polarization (Fig. 10). At lower field strengths two differences were noted in the orientation response. First, the initiation of this response was observed later as the field strengths were decreased. A significant change in orientation was not detected until 20 min after field application at 400 mV/mm, and not until 30 min at 200 mV/mm. Second, the time needed to reach maximal response was longer the lower the field strength, and the degree of polarization was progressively less. Moreover, the response appeared to be nearly linear with time for low field strengths and distinctly nonlinear for higher field strengths.

Since the 90-min time-period chosen was somewhat arbitrary, several longer experiments were carried out (Table III). These indicated that the threshold field in F12 was at least as low as 100 mV/mm for a 3-h period, and that the average polarization appeared to increase with time in some cases. Three of these extended time studies are included in Fig. 10, and both the 300- and 500-mV/mm field strengths resulted in a slightly increased polarization when the cells were exposed for longer times.

Since quail somitic fibroblasts do not move very rapidly in culture (average speed is 0.8 μm/min), we were intrigued by the very rapid, 5-min initiation of the reorientation that occurred when the larger fields were applied. Time-lapse video analysis revealed the apparent cause of this rapid onset of reorientation. We found that cell processes directed towards the positive pole are rapidly retracted into the cell body beginning ~4 min after application of the field (Fig. 11). If the cells have several processes directed towards the positive pole, the process most tangential to the field lines was generally the first to be retracted. In control fields where no current was passed over the cells, the processes were retracted randomly over the course of observation. Eventually, all processes directed toward the anode were retracted. As a result, the remaining cell processes were generally directed perpendicular to the field lines. Some processes still remained extended towards the negative pole, but many of these were lost with longer time in culture, possibly due to the stretching response of the cells (see below), or were converted later into lamellipodia (see Fig. 7). In some cases cells that were not precisely perpendicular to the field will readjust their position later by lamellipodial-directed movement. The threshold for this retraction phenomenon was around 400 mV/mm (Fig. 11) since below this field strength retraction appeared random.

Elongation

At field strengths of 400 mV/mm or greater there was also an elongation response that resulted in longer, thinner cells. The average length of these cells after 48 h in culture was ~80 μm. However, after ~1 h in a field of 400 mV/mm or greater this length began to increase to ~90 μm (Fig. 12). In the lower field strengths this elongation was not observed. Instead the cells actually shortened slightly. This stretching response was

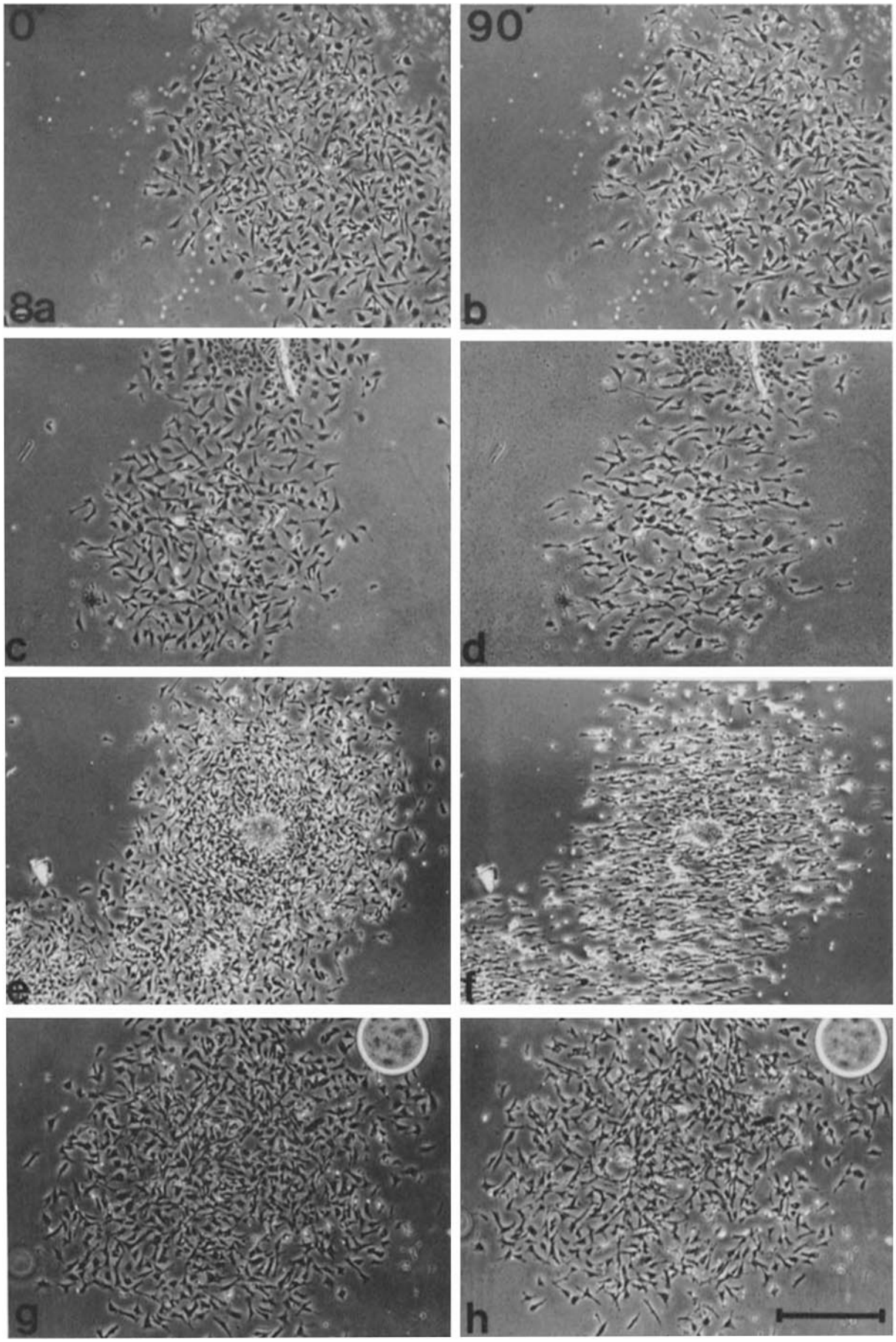
0°
8a
90°
b
c
d
e
f
g
h

TABLE I

Speed of Movement in DC Electric Fields

Field strength	Average speed	Field strength*	p	T	Degrees of freedom
mV/mm	*μm/min*‡	*mV/mm*			
0	0.82 ± 0.31	400	<0.1§	1.62	74
	(31)	500	<0.001	5.04	83
		600	<0.001	4.07	78
50	0.75 ± 0.25	400	<0.01	2.52	80
	(46)	500	<0.001	6.68	81
		600	<0.001	6.06	120
200	0.82 ± 0.36	400	<0.1§	1.35	73
	(33)	500	<0.005	4.59	82
		600	<0.005	3.62	72
400	0.93 ± 0.38	500	<0.005	3.31	98
	(46)	600	<0.01	2.35	104
500	1.26 ± 0.48	‖			
	(53)				
600	1.13 ± 0.42	‖			
	(74)				

Speed of movement is calculated from displacement values over 10-min intervals. Values in parentheses represent the number of cells. The difference between the average speeds was tested for significance using Student's t-test and assuming unknown and unequal variances. The level of significance for the t-test is given by the P-value.

* Speed significantly different from field strength.

‡ ± SD.

§ Marginally significant.

‖ See above for *0, 50, 200, 400 mV/m.*

predicted after our observations of the angle of lamellipodium extension (Fig. 6) which showed a larger number of lamellipodia at 90° and 270° than elsewhere on the cell except at 0°, facing the cathode.

DISCUSSION

New Findings

We have discovered a remarkable example of embryonic fibroblast galvanotaxis in which physiological DC electric fields influenced direction of migration, cell orientation, and cell shape. As we stated in a preliminary report of this phenomenon (30), this is the first example of galvanotaxis in embryonic cells and only the second case of perpendicular orientation (the first being *Xenopus* muscle cell elongation [16]). Recently, two other laboratories have independently found that amphibian neural crest cells exhibit the same three types of response to steady fields (40, 7), and we have also observed the orientation response in quail neural crest cells (12, 30). A third embryonic cell type that has recently been found to exhibit this perpendicular orientation response is the *Xenopus* epithelial cell (26), although galvanotaxis towards the cathode is only observed at very high field strengths.

TABLE II

Average Polarization of Fibroblasts after 90 Min in Indicated Field Strength and Medium

Field strength	Polarization*	Probability that distribution is random
mV/mm		
F-12 medium		
0	−0.08 ± 0.05 (176)	0.17
0	−0.01 ± 0.04 (255)	0.98
0	−0.08 ± 0.07 (106)	0.46
40	−0.04 ± 0.04 (300)	0.10
73	0 ± 0.05 (218)	0.87
93	−0.04 ± 0.05 (211)	0.08
160	0.17 ± 0.06 (128)	0.03
180	0.20 ± 0.04 (264)	10^{-5}
200	0.36 ± 0.04 (230)	10^{-14}
200	0.41 ± 0.04 (271)	10^{-20}
220	0.33 ± 0.05 (189)	10^{-9}
300	0.26 ± 0.04 (270)	10^{-10}
300	0.34 ± 0.04 (261)	10^{-14}
325	0.57 ± 0.03 (281)	10^{-41}
366	0.47 ± 0.03 (330)	10^{-35}
400	0.63 ± 0.03 (235)	10^{-42}
400	0.62 ± 0.03 (217)	10^{-38}
450	0.66 ± 0.03 (266)	10^{-51}
500	0.78 ± 0.02 (260)	10^{-99}
500	0.61 ± 0.03 (243)	10^{-41}
550	0.92 ± 0.01 (196)	10^{-99}
600	0.80 ± 0.03 (196)	10^{-56}
600	0.81 ± 0.02 (200)	10^{-56}
600	0.86 ± 0.02 (173)	10^{-57}
700	0.87 ± 0.02 (157)	10^{-53}
800	0.81 ± 0.03 (151)	10^{-44}
Chick plasma		
0	0 ± 0.05 (201)	0.20
0	0.05 ± 0.04 (249)	0.39
25	0.02 ± 0.05 (182)	0.89
25	0.03 ± 0.04 (250)	0.06
50	0.01 ± 0.05 (191)	0.23
50	0.09 ± 0.05 (225)	0.15
50	0.05 ± 0.06 (157)	0.66
50	0.10 ± 0.04 (248)	0.02
50	0.14 ± 0.05 (174)	0.002
100	0.17 ± 0.05 (173)	0.006
100	0.15 ± 0.04 (244)	0.002
200	0.35 ± 0.04 (266)	10^{-15}
200	0.14 ± 0.04 (258)	0.005
400	0.57 ± 0.03 (230)	10^{-35}
400	0.58 ± 0.03 (232)	10^{-34}
400	0.57 ± 0.03 (230)	10^{-35}
500	0.73 ± 0.03 (230)	10^{-56}
600	0.77 ± 0.02 (232)	10^{-61}
600	0.88 ± 0.02 (156)	10^{-53}

* ± SEM; values in parentheses indicate the number of cells.

FIGURE 8 Micrographs of the same field of 48-h quail somite fibroblasts taken before and after electric field application. In all micrographs the field lines are vertical with the cathode at the top of the photograph. All are in F12 medium except *c* and *d*, which are in plasma. (*a* and *b*) Before and after 90 min in a 200-mV/mm DC electric field. Some reorientation of the cells can be detected. (*c* and *d*) Before and after 90 min in a 400-mV/mm DC field. These cells have become more obviously aligned perpendicular to the field lines. (*e* and *f*) Before and after 90 min in a 600-mV/mm field. Nearly all of the cells are aligned perpendicular to the field. Note also that the cells have elongated more than those at lower field strengths. (*g* and *h*) Before and after 90 min in an AC field of 1,200 mV/mm peak-to-peak at 60 Hz. Bar, 500 μm. × 36.

TABLE III

Average Polarization of Fibroblasts under Various Conditions or Longer Field Applications

Field strength (mV/mm)	Polarization*	Probability that the distribution is random	Duration of field min
Alternating current			
1,200 ptp (60 Hz)	0 ± 0.04 (268)	0.91	90
1,200 ptp (60 Hz)	0.04 ± 0.04 (283)	0.66	90
600 ptp (88 Hz)	−0.03 ± 0.04 (263)	0.83	90
600 ptp (88 Hz)	0.08 ± 0.05 (216)	0.07	90
Hanks' saline medium			
548	0.72 ± 0.03 (301)	10^{-99}	62
450–600	0.81 ± 0.02 (224)	10^{-64}	127
600	0.66 ± 0.04 (136)	10^{-28}	90
Cross-current fluid flow			
600	0.58 ± 0.04 (263)	10^{-39}	90
600	0.73 ± 0.03 (230)	10^{-34}	90
330	0.31 ± 0.04 (226)	10^{-10}	90
Collagen gel embedded			
505	0.80 ± 0.02 (127)	10^{-36}	128
600	0.68 ± 0.04 (137)	10^{-28}	90
Extended times of field application			
15	0.05 ± 0.05 (236)	0.54	180
25	−0.11 ± 0.05 (176)	0.08	240
25	0.02 ± 0.06 (155)	0.86	240
25	0.11 ± 0.05 (237)	0.06	240
50‡	0.14 ± 0.05 (174)	0.002	240
100	0.16 ± 0.04 (249)	10^{-4}	195
150	0.04 ± 0.05 (181)	0.40	180
200‡	0.21 ± 0.04 (216)	10^{-5}	150
300	0.34 ± 0.04 (264)	10^{-15}	150
300	0.28 ± 0.04 (270)	10^{-10}	176
445	0.81 ± 0.02 (224)	10^{-64}	127
500	0.84 ± 0.02 (256)	0	180
505	0.80 ± 0.02 (127)	10^{-36}	128
725	0.85 ± 0.02 (273)	0	95

* ± SEM; values in parentheses indicate number of cells.
‡ In plasma.

Galvanotaxis was not observed in dissociated chick embryo mesoderm cells (39). However this negative result must be viewed with some caution because the 1-mm-high chamber used is likely to heat the cells since resistive heating is proportional to the cross-sectional area of the current path. In fact, quail fibroblasts begin to round up and detach when our chamber height exceeds 200 μm. Moreover, the cells shown in Fig. 4 of that paper do not appear to be well spread and healthy.

The most exciting aspect of our results is the extremely low threshold for the galvanotaxis response of ~1 mV/mm. Much larger fields than this have already been measured beneath the epithelium near a small wound (3), and, as discussed below, it is very likely that embryonic electrical fields of this magnitude are present during the stage in development when these fibroblasts migrate out of the sclerotome.

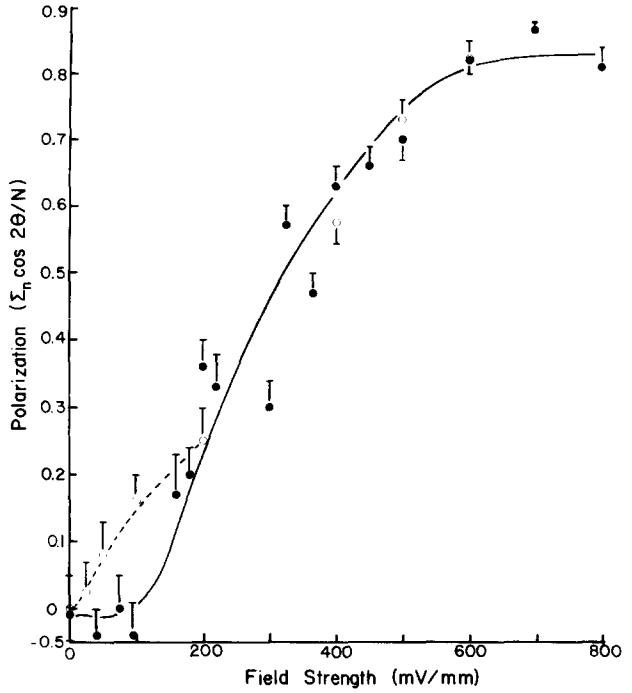

FIGURE 9 Average polarization in the orientation of a population of fibroblasts after 90 min in a DC electric field at the indicated field strength in F12 (●) and chicken plasma (○). Each point represents the average cos 2Θ for 150–300 cells, and the bars indicate SEM. Cells are maximally polarized at ~600 mV/mm in both F12 and in plasma, but the threshold for this response appears to be lower in plasma (50 mV/mm) than in F12 (150 mV/mm).

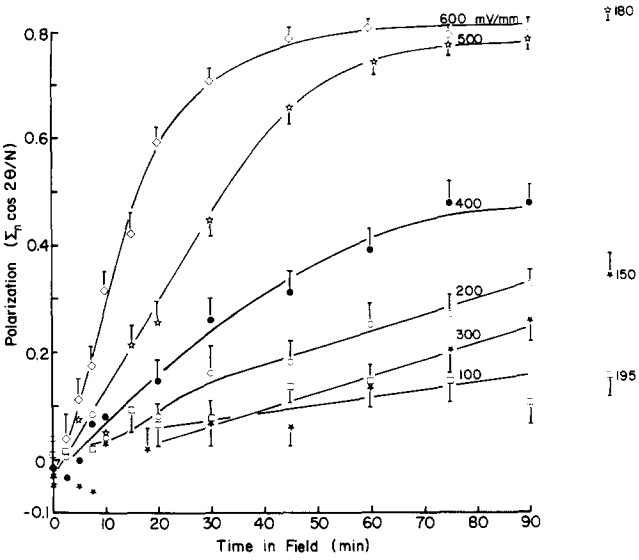

FIGURE 10 Average polarization of a population of fibroblasts in the indicated DC field strength with respect to time. The 100-, 300-, and 500-mV/mm experiments were conducted for extended time periods and the final polarization is plotted on the far right with the measurement time in minutes indicated next to it. Bars represent standard error of the mean (SEM). Note the linearity of the response <400 mV/mm, and the rapid onset of orientation >400 mV/mm.

Other Examples of Cell Galvanotaxis

Studies of galvanotaxis have a long history dating back to the late 1800's when leukocytes and amoebae were first placed in electric fields (9, 44). At least four cell types that normally crawl on substrates have been observed to exhibit galvano-

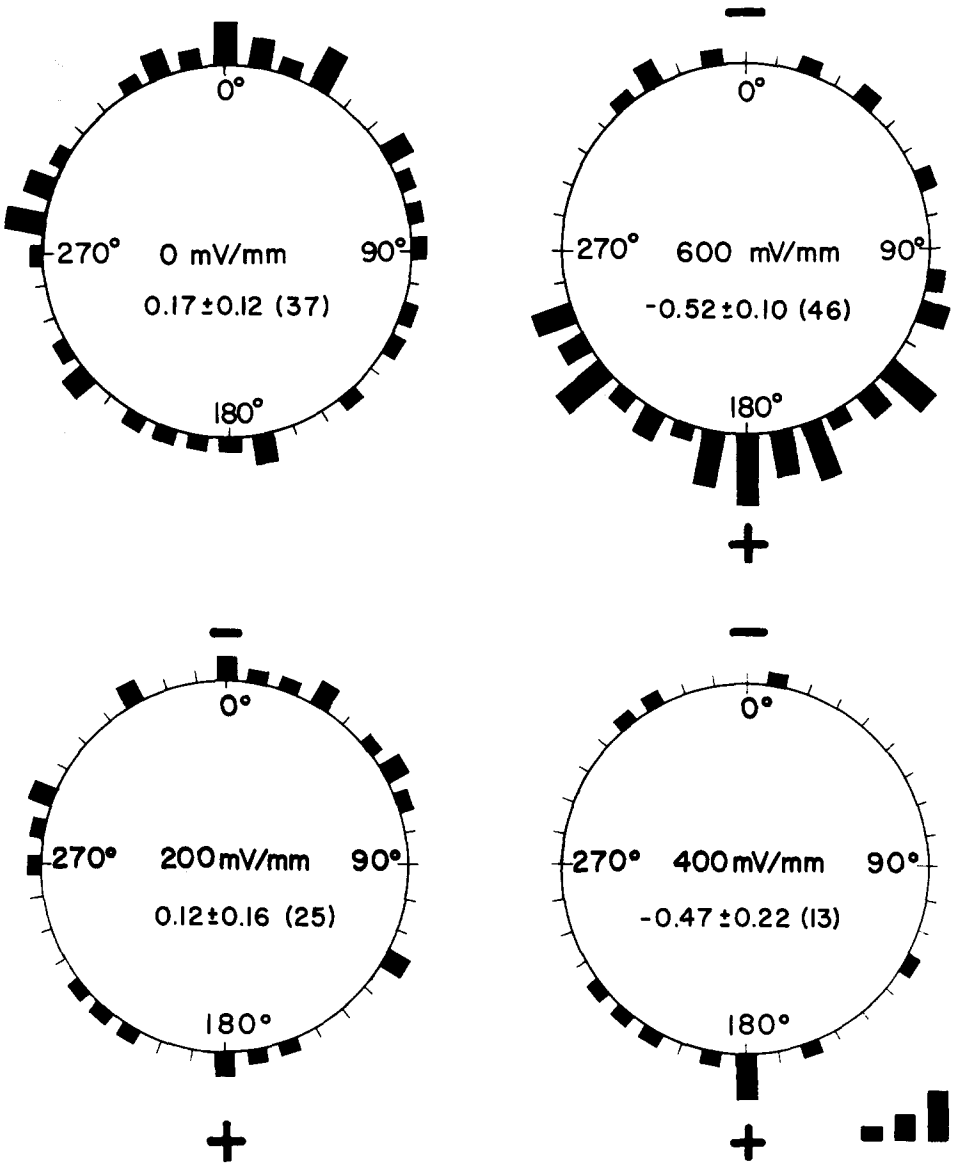

FIGURE 11 This histogram summarizes the orientation of the first process to be retracted after the current was applied as determined from video tapes. 0° represents the cathodal end of the field and 180° is the anodal end. The height of each bar is proportional to the number of processes measured and bar lengths representing one, two, and four cells, respectively, are given on the lower right of the figure. The average cosine of the distribution plus or minus SEM and total cells counted are given below the field strength for each histogram. This average will approach −1 as more cells retract processes facing 180°. In 0- and 200-mV/mm fields processes retract randomly. However, in both the 400- and 600-mV/mm fields the majority of the processes retracted are directed towards the anode. Furthermore, if several processes from one cell are directed towards the anode, the first to be retracted is usually that most nearly aligned with the field lines.

taxis: amoebae, slime molds, leukocytes, and macrophages. Both *Amoeba proteus* and *Physarum polycephalum* migrate towards the cathode with a threshold field strength of 250 and 6 mV/mm, respectively (22, 1). However, the amoeba exhibits only a short-term response, and within a few minutes the cell accommodates to the field and appears to ignore it (37). The amoeba's mean cathodal migration velocity increases linearly with the field strength, but the slime mold's velocity is independent of field strength (1). Both the leukocyte and macrophage migrate toward the anode (29, 14, 31), although it has been reported that in small fields or in regions of inflammation leukocytes move to the cathode (29, 9). Therefore, the embryonic cell galvanotaxis reported here is one of the most persistent behaviors thus far observed.

Why Study Galvanotaxis?

This research was prompted by our speculation that migratory embryonic cells might encounter electric fields in the embryo during normal development. Epithelial layers are well known to pump ions and other solutes across themselves (23). These ion movements are often electrogenic and will generate an ion current across the cell layer that will leak back through regions of low intercellular resistance. Such outward leakage currents of 100 $\mu A/cm^2$ have been detected exiting the primitive streak of early chick embryo (stages three to five) and return elsewhere through the epiblast (20). This current is probably pumped into the intraembryonic space by the epiblast and then leaks out of the streak because it is a zone of junctional disruption. It will generate a voltage gradient across some ingressing cells, and the magnitude of this gradient will depend on the resistivity of the embryonic spaces through which the current flows. Similar large current densities leave the neural tube in *Xenopus* embryos (36). Again, these currents appear to be driven by a pumping epithelium. The potential difference across the skin of the adult frog has been extensively studied (23), and recently McCaig and Robinson (27) have shown that this transepidermal potential difference first begins to appear at neurulation. However, no gradients in skin potential within the embryo that might influence nerve

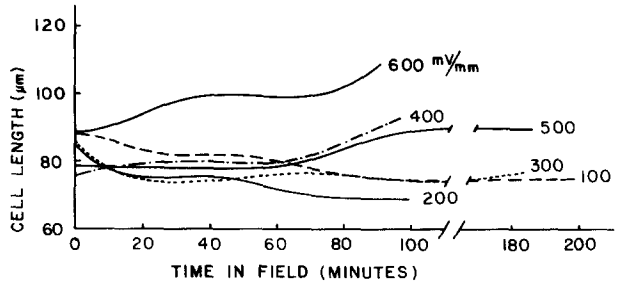

FIGURE 12 Average fibroblast length versus time in the indicated DC electric fields. At field strengths of 400 mV/mm or greater the cells begin to elongate after a variable time lag. At field strengths of 300 mV/mm or less, the cells actually appear to shorten somewhat with time in the field.

or muscle growth have thus far been detected. We have made preliminary extracellular current measurements around quail embryos and also measured large currents exiting the neuropore and entering along the epiblast. Furthermore, our preliminary measurements indicate that the neural tube is itself an epithelium that is generating ion currents and local electric fields. These currents will generate voltage gradients within the embryo that will be proportional to the local resistivity. This resistivity will depend on the nature of the cell-cell junctions and the extracellular matrix in the region, but an average tissue resistivity is on the order of 1,000 Ω-cm (38). Using this resistivity value, the measured embryonic current density of 100 $\mu A/cm^2$ would generate an internal voltage gradient of 10 mV/mm, which is above the threshold field observed in this report. The only direct measurements of natural voltage gradients have been made recently by Barker et al. (3) beneath the epithelial layer near a wound in guinea pig skin. When an incision is made through the glabrous epidermis, a microampere flows through each millimeter of the cut's edge. These wound currents generate lateral, intraepidermal voltage gradients of ~200 mV/mm near the cut. Since this is ~100-fold greater than the threshold field for fibroblast galvanotaxis, we believe that the field strengths used in our study encompass a physiological range.

Possible Mechanisms for this Electric Field Sensitivity

Since this galvanotaxis response occurred in protein-free saline or with a perpendicular cross-current flow, the field appears to be exerting a direct influence on the cells themselves rather than acting indirectly on the cells by establishing an external protein gradient, for example. When these fibroblasts adhere to a glass substratum and are placed in an electric field, a uniform current will flow over the tops of the flattened cells, generating a linear voltage gradient along this upper surface. Since the plasma membrane poses a large resistance to current flow, only a small fraction of the current will enter the cell to generate a cytoplasmic voltage gradient. In fact, one can calculate that the cytoplasmic voltage gradient through the interior of a cell would be only 10^{-5}–10^{-3} times the total voltage gradient across that cell (18). Nearly the entire voltage gradient across the cell is found across the membranes facing each pole of the field. A cell placed in a constant field of 10 mV per cell length will "feel" approximately half of that voltage across each membrane facing the poles, resulting in a 5-mV depolarization at the cathodal end of a 5-mV hyperpolarization at the anodal end. Thus, the most likely immediate target of an imposed field is the plasma membrane. The field will impose a local membrane potential perturbation and will also generate the previously mentioned lateral voltage gradient along the upper membrane surface.

Membrane potential perturbations might influence the orientation or function of integral membrane proteins. For example, they are well known to affect ion permeabilities via voltage-sensitive protein ion channels. Such Na^+, K^+, Ca^{2+}, and Cl^- channels are thought to be responsible for all action potentials. The threshold for these action potentials is generally a 15–20-mV depolarization, but it is possible that a smaller potential perturbation might increase the probability for a brief period in the open state. Some experimental support for this notion has been found in mouse peritoneal macrophages placed in a steady electric field (31). Fields >400 mV/mm (~10 mV per cell diameter) stimulate pseudopodial protrusive activity toward the positive pole. This response is dependent on extracellular Ca^{2+} and can be blocked by Ca^{2+} influx inhibitors. Therefore it is possible that the local membrane potential perturbation (in this case a hyperpolarization) is acting to increase the local Ca^{2+} influx. The subsequent rise in internal free Ca^{2+} might then influence pseudopodium formation. However, since motility itself is often dependent on external Ca^{2+}, these effects of Ca^{2+} inhibitors may be blocking galvanotaxis only secondarily. A similar line of evidence has been derived from studies of fresh-water amoebae. These cells were injected with the Ca^{2+}-sensitive photoprotein, aequorin. Pulsed electric field application across such cells (~50–500 mV/cell) is accompanied by simultaneous increases in Ca^{2+} at the anodal side indicating local stimulated Ca^{2+} entry again at the hyperpolarized end (41). This only occurs at a much larger field strength than we have used here, however.

Lateral voltage gradients along the top surface of the cell might influence the distribution of membrane proteins by lateral electrophoresis. This mechanism for generating membrane asymmetry was first proposed by Jaffe in 1977 and has since been demonstrated in various cells (35, 34). Direct evidence for this lateral electrophoresis in motile cells has been found in macrophages where both Con A and *Phaseolus vulgaris* lectin receptors are redistributed by imposed fields to opposite ends of the cell. Although such a membrane receptor segregation might well be driven by some nonelectrophoretic mechanism, similar membrane receptor movements in other cells placed in electric fields have been found to be independent of cellular ATP as well as microfilaments and microtubules (32), and quite sensitive to surface charge as would be expected if electrophoresis were involved (34). Growing *Xenopus* neurons in culture exhibit a similar lateral electrophoresis of Con A receptors that is important for the negative galvanotropism. Incubation in 40 μg/ml Con A during field application blocks Con A receptor migration and also blocks the galvanotropic response completely.

The earliest response that we observed, that of process retraction, is most likely due to the membrane potential perturbation because it occurs preferentially in cells aligned with the field that will experience a 24-mV change across each membrane facing the poles in a 600-mV/mm field. Furthermore, this response is not observed in fields below 400 mV/mm, and it normally occurs within 5–10 min of field application which is too soon for any significant lateral electrophoresis (34). On the other hand, the cell migration response exhibits a very low threshold of ~1 mV/mm in plasma and

this would impose only a 10-μV perturbation of the membrane potential across a cell's width, and a 40-μV perturbation along the length. This would be a very small membrane potential perturbation in a typical cell with a −70-mV membrane potential, but it is very difficult to distinguish between the two mechanisms based on these data.

This manner of locomotion where cells extend lamellipodia perpendicular to their long axes in the electric field is not a commonly observed form of motility in tissue culture, so one might question the significance of this aspect of the cells' behavior. Three points should be considered here. First, this sideways crawling was not as predominant in cells placed in the lower fields near the threshold for perpendicular alignment that still stimulated translocation toward the cathode (see Fig. 3*b*). In fact, the threshold for directed migration is at least an order of magnitude lower than the threshold for perpendicular orientation. Thus, the absence of such orientation in vivo may be due to lower natural field strengths. Second, there are indeed several examples of this mode of movement in the literature, both in vivo and in vitro, so these movements are not unique to these cells. Cells that exhibit this mode of motility have sometimes been referred to as "canoe" cells due to their shape and include *Fundulus* mesenchyme and epidermal cells (15, 2, 21), mammalian kidney epithelial cells (21), *Xenopus* epidermal cells (4), and chicken heart fibroblasts (21). Therefore this mode of fibroblast movement observed in electric fields is not totally without precedent. Third, orientation of the cell axis can be influenced by contact guidance (45, 10) of aligned substratum material such as collagen. It is possible that aligned collagen in the embryo (24) most strongly influences cell orientation whereas the electric field controls the direction of migration. It will be most interesting to determine whether currents of the appropriate magnitude and orientation to direct fibroblast migration exist around the neural tube at the time that these cells initiate their migration.

This galvanotactic response should also be useful for the study of cell motility mechanisms. Since this response clearly separates three components of cell movement, orientation, elongation, and translocation, it should be possible to study the mechanisms involved in each. In particular, field application separates the axis of polarity from the axis of migration and can be used to determine which organelles (e.g. Golgi apparatus, microtubule-organizing center) are associated with migration and which with the axis of polarity.

We thank Lionel Jaffe and Ken Robinson for helpful discussions during these experiments. We are particularly indebted to Ron Smith for writing most of our computer programs and helping with data analysis. We also thank Tanya Feige for photographic assistance.

This work was supported by National Science Foundation grant PCM 81 18174 and National Institutes of Health grant K04 HDO 0470 to R. Nuccitelli, and National Science Foundation grant PCM 8004524 and National Institutes of Health grant PHS DE05630 to C. A. Erickson.

Received for publication 6 June 1983, and in revised form 6 September 1983.

REFERENCES

1. Anderson, J. D. 1951. Galvanotaxis of slime mould. *J. Gen. Physiol.* 35:1–11.
2. Armstrong, P. B. 1980. Time-lapse cinemicrographic studies of cell motility during morphogenesis of the embryonic yolk sac of *Fundulus heteroclitus* (Pisces Teleosti). *J. Morphol.* 165:13–29.
3. Barker, A. T., L. F. Jaffe, and J. W. Vanable, Jr. 1982. The glabrous epidermis of cavies contains a powerful battery. *Am. J. Physiol.* 242:R358–R366.
4. Bereiter-Hahn, J., R. Strohmeier, I. Kunzenbacher, K. Beck, and M. Voth. 1981. Locomotion of *Xenopus* epidermis cells in primary culture. *J. Cell Sci.* 52:289–311.
5. Borgens, R. B., J. W. Vanable, Jr., and L. F. Jaffe. 1977. Bioelectricity and regeneration: large currents leave the stumps of regenerating newt limbs. *Proc. Natl. Acad. Sci. USA.* 74:4528–4532.
6. Chen, W.-T. 1979. Induction of spreading during fibroblast movement. *J. Cell Biol.* 81:684–691.
7. Cooper, M. S., and R. E. Keller. 1982. Electrical currents induce perpendicular orientation and cathode-directed migration of amphibian neural crest cells in culture. *J. Cell Biol.* 95:323a.
8. Curray, J. R. 1956. The analysis of two-dimensional orientation data. *J. Geol.* 64:117–130.
9. Dineur, E. 1891. Note sur la sensibilité des leucocytes a l'electricité. *Bulletin Seances Soc. Belge Microscopie (Bruxelles).* 18:113–118.
10. Dunn, G. A. 1982. Contact guidance of cultured tissue cells: a survey of potentially relevant properties of the substratum. *In* Cell Behaviour. R. Bellairs, A. Curtis, and G. Dunn, editors. Cambridge University Press, Cambridge. 471–498.
11. Elsdale, T., and J. Bard. 1972. Collagen substrate for studies on cell behaviour. *J. Cell Biol.* 54:626–637.
12. Erickson, C. A., and R. Nuccitelli. 1982. Embryonic cell motility can be guided by weak electrical fields. *J. Cell Biol.* 95(2, Pt. 2):314 *a.* (Abstr.)
13. Freeman, J. A., J. M. Weiss, G. J. Snipes, B. Mayes, and J. J. Norden. 1981. Growth cones of goldfish retinal neurites generate DC currents and orient in an electric field. *Soc. Neurosciences Abstracts.* 1:550.
14. Fukushima, K., N. Senda, H. Inui, H. Miura, Y. Tamai, and Y. Murakami. 1953. Studies on galvanotaxis of leukocytes. I. Galvanotaxis of human neutrophilic leukocytes and methods of its measurement. *Med. J. Osaka Univ.* 4:195–208.
15. Goodrich, H. B. 1924. Cell behavior in tissue cultures. *Biol. Bull. (Woods Hole).* 46:252–262.
16. Hinkle, L., C. D. McCaig, and K. R. Robinson. 1981. The direction of growth of differentiating neurones and myoblasts from frog embryos in an applied electric field. *J. Physiol.* 314:121–135.
17. Jaffe, L. F. 1977. Electrophoresis along cell membranes. *Nature (Lond.).* 265:600–602.
18. Jaffe, L. F., and R. Nuccitelli. 1977. Electrical controls of development. *Annu. Rev. Biophys. Bioeng.* 6:445–476.
19. Jaffe, L. F., and M.-m. Poo. 1979. Neurites grow faster towards the cathode than the anode in a steady field. *J. Exp. Zool.* 209:115–128.
20. Jaffe, L. F., and C. D. Stern. 1979. Strong electrical currents leave the primitive streak of chick embryos. *Science (Wash. DC).* 206:569–571.
21. Kolega, J., M. S. Shure, and W.-T. Chen. 1982. Rapid cellular translocation is related to close contacts formed between various cultured cells and their substrata. *J. Cell Sci.* 54:23–34.
22. Korohoda, W., and A. Kurowska. 1970. Quantitative estimations of the thresholds of electrotactic responses in *Amoeba proteus. Acta. Protozool.* 7:375–382.
23. Lindemann, B., and C. Voute. 1976. Structure and function of the epidermis. *In* Frog Neurobiology. R. Llinas and W. Precht, editors. Springer-Verlag, New York. 169–210.
24. Löfberg, J., K. Ahlfors, and C. Fallstrom. 1980. Neural crest cell migration in relation to extracellular matrix organization in the embryonic axolot trunk. *Dev. Biol.* 75:148–167.
25. Loring, J., B. Glimelius, C. Erickson, and J. A. Weston. 1981. Analysis of developmentally homogeneous neural cell populations *in vitro. Dev. Biol.* 82:86–94.
26. Luther, P. W., H. B. Peng, and J. J.-C. Lin. 1983. Changes in cell shape and actin distribution induced by constant electric fields. *Nature (Lond.).* 303:61–64.
27. McCaig, C. D., and K. R. Robinson. 1982. The ontogeny of the transepidermal potential difference in frog embryos. *Dev. Biol.* 90:335–339.
28. Meech, R. W. 1978. Calcium-dependent potassium activation in nervous tissues. *Annu. Rev. Biophys. Bioeng.* 7:1–18.
29. Monguio, J. 1933. Uber die polare Wirkung des galvanischen Stromes auf Leukozyten. *Z. Biol.* 93:553–559.
30. Nuccitelli, R., and C. A. Erickson. 1983. Embryonic cell motility can be guided by physiological electric fields. *Exp. Cell Res.* 147:195–201.
31. Orida, N., and J. D. Feldman.1982. Directional protrusive pseudopodial activity and motility in macrophages induced by extracellular electric fields. *Cell Motility.* 2:243–255.
32. Orida, N. and M.-m. Poo. 1978. Electrophoretic movement and localization of acetylcholine receptors in embryonic muscle cell membrane. *Nature (Lond.).* 275:31–35.
33. Patel, N., and M.-m. Poo. 1982. Orientation of neurite growth by extracellular electric fields. *J. Neuroscience.* 2:483–496.
34. Poo, M.-m. 1981. *In situ* electrophoresis of membrane components. *Annu. Rev. Biophys. Bioeng.* 10:245–276.
35. Poo, M.-m., and K. R. Robinson. 1977. Electrophoresis of concavalin A receptors along embryonic muscle cell membrane. *Nature (Lond.).* 265:602–605.
36. Robinson, K. R., and R. F. Stump. 1983. Self generated electrical currents through neurulae. *J. Physiol. (Lond.).* In press.
37. Sayers, Z., A. M. Roberts, and L. H. Bannister. 1979. Random walk analysis of movement and galvanotaxis of *Amoeba proteus. Acta. Protozool.* 18:313–325.
38. Schwan, H. P. 1963. Electric characteristics of tissues. *Biophysik.* 1:198–208.
39. Stern, C. D. 1981. Behaviour and motility of cultured chick mesoderm cells in steady electrical fields. *Exp. Cell Res.* 136:343–350.
40. Stump, R. F., and K. R. Robinson. 1982. Directional movement of *Xenopus* embryonic cells in an electric field. *J. Cell Biol.* 95(2, Pt. 2):331 *a.* (Abstr.)
41. Taylor, D. L., G. T. Reynolds, and R. D. Allen. 1975. Detection of free calcium ions in amoebae by aequorin luminescence. *Biol. Bull. (Woods Hole).* 149:448.
42. Trinkaus, J. P. 1976. On the mechanism of metazoan cell movements. *In* The Cell Surface in Animal Embryogenesis and Development. G. Poste and G. I. Nicolson, editors. North-Holland, Amsterdam. 226–329.
43. Trinkaus, J. P. 1982. Some thoughts on directional cell movement during morphogenesis. *In* Cell Behaviour. R. Belliars, A. Curtis, and G. Dunn, editors. Cambridge University Press, Cambridge. 471–498.
44. Verworn, M. 1896. Untersuchungen uber die polare Erregung der lebendigen Substanz durch den konstanten Strom. III. Mitteliung. *Pflugers Arch. Eur. J. Physiol.* 62:415–450.
45. Weiss, P. 1934. *In vitro* experiments on the factors determining the course of the outgrowing nerve fiber. *J. Exp. Zool.* 68:393–448.